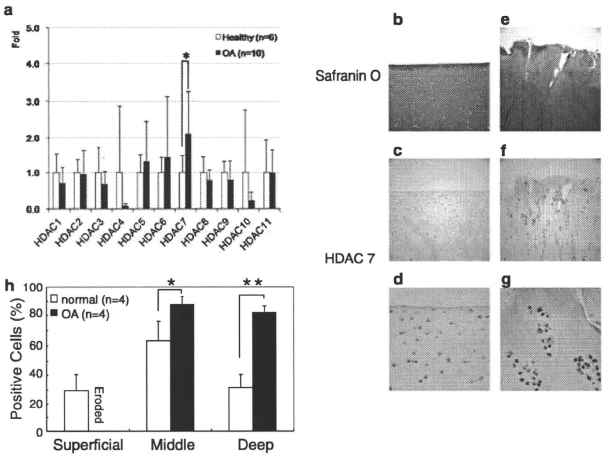

Fig. 2 Localization of HDAC7 in normal and OA knee cartilage. **a** HDAC1–11 mRNA expression in human knee cartilage was determined by real-time RT-PCR. In normal samples, HDAC3 was the most abundantly expressed HDAC (data not shown). HDAC7 had significantly higher expression in OA than in normal cartilage (Fig. 2a). Cartilage was obtained from 6 normal donors (mean age 30.8 years; range 19–49 years; Mankin score 0–2 points) and 10 OA donors (mean age 71.6 years; range 44–93 years old; Mankin score 5–10 points) (Fig. 2a). The results are expressed as mean ± SD. $*P < 0.05$. **b–g** HDAC7 localization was examined in tissue from 4 normal donors (age range 19–48 years) and 4 OA donors (age range 48–93 years). HDAC7-positive cells were more frequent in OA cartilage than in normal cartilage. The immunoreactive product is *dark red*. ×10 (**b**, **c**, **e**, **f**). **h** The number of HDAC7-positive cells was counted in the superficial, middle, and deep zones of sections from normal ($n = 4$) and OA ($n = 4$) cartilage with specific antibodies. The OA middle and deep zones had significantly more HDAC7-positive cells than did normal middle and deep zones, respectively. The results are expressed as mean ± SD. $*P < 0.05$, $**P < 0.01$

normal chondrocytes, we used SW1353 human chondrosarcoma cells for this assay (data not shown).

Quantitative polymerase chain reaction

Total RNA was isolated from cartilage tissues or monolayer chondrocyte cultures using Trizol (Invitrogen Inc., Carlsbad, CA, USA). Complementary DNA was produced using Ready-To-Go You Prime First Strand Beads (GE Health Inc., USA) with 2 μg total RNA and oligo (dT) primers. Messenger RNA expression of HDAC1–11 and MMP-13 was detected by real-time RT-PCR with TaqMan Gene Expression Assay probe (Applied Biosystems Inc.) using an iCycler (Bio-Rad Laboratories Inc., Hercules, CA, USA) as follows: 10 min at 95°C for initial denaturation, followed by 45 cycles at 95°C (15 s) and 60°C (1 min). The expression levels of HDACs and MMP-13 were defined from the threshold cycle (Ct) and relative values were calculated by the $2^{-\Delta\Delta Ct}$ method after normalizing expression to GAPDH.

Histology and immunohistochemistry

Cartilage tissues were fixed with 4% paraformaldehyde and stained with Safranin O. HDAC7 antibodies were purchased from Santa Cruz Biotechnologies (catalog no. sc-11421, Santa Cruz, CA, USA). Paraffin-fixed samples were first deparaffinized in xylene substitute Pro-Par Clearant (Anatech Ltd, Battle Creek, MI, USA) and ethanol before rehydration in water. Following a wash with phosphate-buffered saline (PBS), sections were blocked with 0.1% Tween 20 with 3% normal goat serum for 30 min at room temperature. HDAC7 antibodies (1:50 dilution; 4 μg/mL) and normal rabbit immunoglobulin G (IgG, 4 μg/mL) as a negative control were applied and incubated overnight at 4°C. After washing with PBS, sections were incubated with biotinylated goat anti-rabbit secondary antibody for 30 min (1:200; Vector Laboratories Inc., Burlingame, CA, USA) and then incubated with Vectastain ABC-AP kit (AK-5000; Vector Laboratories Inc., Burlingame, CA, USA) for 30 min at room temperature. Finally, sections

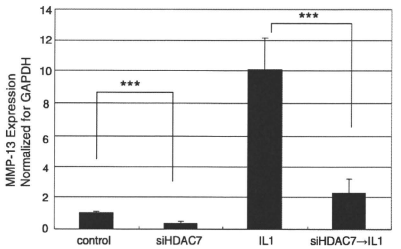

Fig. 3 Knockdown of HDAC7 by siRNA in SW1353 human chondrosarcoma cells. Real-time PCR results of MMP-13 expression in HDAC7 knocked down cells with and without the additional 5 h of culturing in IL-1 (5 ng/mL). Knockdown of HDAC7 decreased both natural and IL-1-induced MMP-13 expression. Data are presented as mean ± SD ($n = 2$, in duplicate). ***$P < 0.001$

were stained with an alkaline phosphatase substrate kit (Vector Laboratories Inc., Burlingame, CA, USA).

Quantification and localization of signals throughout cartilage

To systematically assess HDAC7 localization throughout each cartilage zone, we counted positive and negative cells in a 50 × 50 μm^2 grid (using a 40× field objective) starting from the cartilage surface to the deep zone (DZ). This procedure was repeated a minimum of 5 times for each section. We based our identification of each zone on previously reported characteristics that comprise cell shape, morphology, orientation, and pericellular matrix (PM) deposition [27]. Thus, superficial zone (SZ) cells were characterized by their elongated shape, their parallel orientation relative to the surface, and their lack of extensive PM. These cells predominate within the first 50 μm. The middle zone (MZ) was distinguishable by the presence of rounded cells without an organized orientation relative to the surface, an extracellular matrix (ECM) rich in proteoglycans, and evidence of PM. Conversely, DZ cells were recognized by extensive PM deposition and an organization of 3 or more cells in chondron groups arranged in columns. The depth of each zone was recorded for each section for comparative analysis on the frequency of positive signals in each zone. The frequency of positive cells was expressed as a percentage relative to the total number of cells counted in each zone.

Statistical analysis

Statistically significant differences between 2 groups were determined with t tests. Results are presented as mean ± standard deviation (SD). P values of less than 0.05 were considered statistically significant.

Results

Histone deacetylase inhibitor TSA modulates MMP-13 gene expression

To examine the potential role of HDACs on MMP13 expression, chondrocytes were treated with TSA, a HDAC inhibitor. We used normal chondrocytes ($n = 6$) to exclude effect of OA changes on chondrocytes. When treating human knee chondrocytes with TSA only, natural MMP-13 expression was suppressed to a small degree ($P = 0.120$) and with IL-1 induction of MMP-13 the suppression was greater ($P = 0.067$), but none of the results were statistically significant (Fig. 1). Even though not significant, these results provide a clue and increase our curiosity to which HDAC is affecting the MMP-13 expression.

HDAC7 expression is elevated in OA cartilage

All the knee cartilage samples obtained for this study were examined for HDAC1–11 messenger RNA (mRNA) expressions in human by real-time PCR. Expression of HDAC7 was significantly higher in OA than in normal cartilage (Fig. 2a). On the other hand, HDAC4 and HDAC10 were relatively lower in OA cartilage, although the changes were not statistically significant.

Normal and OA samples stained with Safranin O (Fig. 2b, e) displayed different localization of HDAC7-positive cells. In normal cartilage, we detected positive cells in the MZ (Fig. 2c), whereas in OA cartilage we detected many positive cells, especially in chondrocyte clusters (Fig. 2f, g). Representative examples were a normal 19-year-old female (Mankin score 1) and a 57-year-old male with OA (Mankin score 9). Figure 2h presents the quantitative analysis of zonal distribution of HDAC7-expressing cells in 4 normal (range 19–48 years old) and OA (range 48–93 years old) donors. Complete erosion of the SZ was observed in OA cartilage. Moreover, significantly more positive cells were observed in middle and DZs in OA cartilage, compared with in normal middle and DZs, respectively.

Knockdown of HDAC7 significantly decreases MMP-13 expression

To investigate the correlation between HDAC7 and MMP-13, HDAC7 was knocked down by siRNA in SW1353 human chondrosarcoma cells and mRNA expression of MMP-13 was measured by real-time RT-PCR. HDAC7

knockdown cells were further stimulated with IL-1, and MMP-13 expression was measured again. Knocking down HDAC7 in SW1353 cells decreased both natural and IL-1-induced MMP-13 expression significantly (Fig. 3), indicating functional interaction between HDAC7 and MMP-13.

Discussion

Onset and progression of OA is associated with changes in chondrocyte gene expression. HDACs balance histone acetyltransferases (HATs) and regulate gene transcription epigenetically, and thereby control the acetylation status of histone proteins and nonhistone substrates. In general, acetylation of histones loosens nucleosomal structures, which promotes gene transcription. In contrast, deacetylation of histones stabilizes nucleosomal structures and represses gene transcription [28, 29]. However, emerging evidence indicates that gene regulation by acetylation/deacetylation is more dynamic and complex, and that HATs also can act as repressors and HDACs as transcription activators. Indeed, global analysis of gene expression has shown that inhibition of HDAC activity results in both induction and repression of gene expression [30–35]. Recent studies demonstrated that HDAC inhibitors have therapeutic effects in cancer and inflammatory diseases [14–23]. Young et al. [22] revealed that HDAC inhibitors modulate MMP gene expression in chondrocytes and block cartilage resorption. Although we could not find a statistically significant difference, there is a tendency for MMP13 to be reduced by TSA treatment. As TSA inhibits multiple HDACs, it may be difficult to see direct effect of specific HDAC inhibition by TSA treatment. In this regard, our data showing that specific reduction of HDAC7 by siRNA inhibited MMP-13 expression (Fig. 3) support the idea that HDAC7 promotes MMP-13 in OA pathogenesis.

Matrix metalloproteinases are a family of enzymes that collectively degrade components of the ECM. They are important in normal physiological processes such as development and wound healing, where they appear in a low concentration. In contrast, aberrant MMP expression occurs in several disease states, including atherosclerosis, tumor invasion, and arthritic diseases [36, 37]. MMPs mediate irreversible matrix degradation and subsequent joint destruction in RA and OA. MMP-13 is expressed by chondrocytes and is critical for collagen degradation as it hydrolyzes type II collagen more efficiently than do other collagenases [38]. Therefore, we wanted to see whether a specific HDAC is responsible for IL-1-induced MMP-13 expression and thus contributes to cartilage degradation in OA.

In the present study, we observed significant upregulation of HDAC7 in OA cartilage by real-time RT-PCR and immunohistochemistry (Fig. 2a). HDAC7 is a member of the class II HDACs, which comprises HDAC4, 5, 6, 7, 9, and 10, all of which display cell-type-restricted patterns of expression and contain a highly conserved C-terminal deacetylase catalytic domain. Class II HDACs also contain an N-terminal extension that links them to specific transcription factors and confers responsiveness to a variety of signal transduction pathways serving as a link between the genome and the extracellular environment [39]. Disruption of the HDAC7 gene in mice results in embryonic lethality due to a failure of endothelial cell–cell adhesion and consequent dilatation and rupture of blood vessels. HDAC7 represses MMP-10 gene transcription by associating with myocyte enhancer factor-2 (MEF2), a direct activator of MMP-10 transcription and an essential regulator of angiogenesis [40].

Recently, Jensen et al. [41] demonstrated that HDAC7 associates with Runx2 and represses its activity during osteoblast maturation. Runx2 is required for MMP-13 promoter activity induced by IL-1 [42]. Increased expression of Runx2 in OA cartilage may contribute to increased expression of MMP-13 [43]. Kawaguchi [44] proposed that endochondral ossification signals, in which Runx2 plays a central role, may be important for OA progression [45]. The expression pattern of HDAC7 is different between normal and OA cartilage and the localization of HDAC7 in OA is similar to Runc2 expression in OA [43], suggesting the potential link between Runx2 and HDAC7 in OA pathogenesis. It will be interesting to test whether HDAC7 and Runx2 may cooperatively regulate MMP13 in chondrocytes.

The human genome contains only 18 HDAC genes, but more than 1,800 genes are predicted to encode transcription factors [46]. Given the number of other mechanisms for regulation of MMP-13 expression [47–53], it is important to identify the precise mechanism for how HDAC7 may regulate MMP-13 via specific transcription factors in OA chondrocytes. On the other hand, it is likely that HDAC7 regulates many other OA-related genes. Based on our current study showing the link between HDAC7 and MMP-13 in OA chondrocytes, it is important to examine other HDAC7 targets in OA pathogenesis and test whether HDAC7 could be a therapeutic target by in vivo study.

Conclusions

Our findings support the idea that HDAC7 expression is elevated in human OA cartilage and promotes IL-1 induction of MMP13, contributing to cartilage degradation. Many enigmatic interactions remain unclear, and further

studies are needed to elucidate the mechanism of cartilage degradation by MMP-13 in OA.

Acknowledgments This study was supported by NIH grants AR056120, AR050631, AG007996, and AG033409.

Conflict of interest statement None.

References

1. Pelletier JP, Martel-Pelletier J, Abramson SB. Osteoarthritis, an inflammatory disease: potential implication for the selection of new therapeutic targets. Arthritis Rheum. 2001;44(6):1237–47.
2. Goldring MB. The role of the chondrocyte in osteoarthritis. Arthritis Rheum. 2000;43(9):1916–26.
3. Goldring MB, Berenbaum F. The regulation of chondrocyte function by proinflammatory mediators prostaglandins and nitric oxide. Clin Orthop Relat Res. 2004;427(suppl):S37–46.
4. Bau B, Gebhard PM, Haag J, Knorr T, Bartnik E, Aigner T. Relative messenger RNA expression profiling of collagenases and aggrecanases in human articular chondrocytes in vivo and in vitro. Arthritis Rheum. 2002;46(10):2648–57.
5. Billinghurst RC, Dahlberg L, Ionescu M, Reiner A, Bourne R, Rorabeck C, et al. Enhanced cleavage of type II collagen by collagenases in osteoarthritic articular cartilage. J Clin Invest. 1997;99(7):1534–45.
6. Neuhold LA, Killar L, Zhao W, Sung ML, Warner L, Kulik J, et al. Postnatal expression in hyaline cartilage of constitutively active human collagenase-3 (MMP-13) induces osteoarthritis in mice. J Clin Invest. 2001;107(1):35–44.
7. Gregoretti IV, Lee YM, Goodson HV. Molecular evolution of the histone deacetylase family: functional implications of phylogenetic analysis. J Mol Biol. 2004;338(1):17–31.
8. de Ruijter AJ, van Gennip AH, Caron HN, Kemp S, van Kuilenburg AB. Histone deacetylases (HDACs): characterization of the classical HDAC family. Biochem J. 2003;370(Pt 3):737–49.
9. Bernstein BE, Tong JK, Schreiber SL. Genomewide studies of histone deacetylase function in yeast. Proc Natl Acad Sci USA. 2000;97(25):13708–13.
10. Mulholland NM, Soeth E, Smith CL. Inhibition of MMTV transcription by HDAC inhibitors occurs independent of changes in chromatin remodeling and increased histone acetylation. Oncogene. 2003;22(31):4807–18.
11. Nair AR, Boersma LJ, Schiltz L, Chaudhry MA, Muschel RJ. Paradoxical effects of trichostatin A: inhibition of NF-Y-associated histone acetyltransferase activity, phosphorylation of hGCN5 and downregulation of cyclin A and B1 mRNA. Cancer Lett. 2001;166(1):55–64.
12. Pujuguet P, Radisky D, Levy D, Lacza C, Bissell MJ. Trichostatin A inhibits beta-casein expression in mammary epithelial cells. J Cell Biochem. 2001;83(4):660–70.
13. Saunders N, Dicker A, Popa C, Jones S, Dahler A. Histone deacetylase inhibitors as potential anti-skin cancer agents. Cancer Res. 1999;59(2):399–404.
14. Lin HY, Chen CS, Lin SP, Weng JR. Targeting histone deacetylase in cancer therapy. Med Res Rev. 2006;26(4):397–413.
15. Villar-Garea A, Esteller M. Histone deacetylase inhibitors: understanding a new wave of anticancer agents. Int J Cancer. 2004;112(2):171–8.
16. Johnstone RW. Histone-deacetylase inhibitors: novel drugs for the treatment of cancer. Nat Rev Drug Discov. 2002;1(4):287–99.
17. Kortenhorst MS, Carducci MA, Shabbeer S. Acetylation and histone deacetylase inhibitors in cancer. Cell Oncol. 2006;28(5–6):191–222.
18. Blanchard F, Chipoy C. Histone deacetylase inhibitors: new drugs for the treatment of inflammatory diseases? Drug Discov Today. 2005;10(3):197–204.
19. Lin HS, Hu CY, Chan HY, Liew YY, Huang HP, Lepescheux L, et al. Anti-rheumatic activities of histone deacetylase (HDAC) inhibitors in vivo in collagen-induced arthritis in rodents. Br J Pharmacol. 2007;150(7):862–72.
20. Nasu Y, Nishida K, Miyazawa S, Komiyama T, Kadota Y, Abe N, et al. Trichostatin A, a histone deacetylase inhibitor, suppresses synovial inflammation and subsequent cartilage destruction in a collagen antibody-induced arthritis mouse model. Osteoarthr Cartil. 2008;16(6):723–32.
21. Nishida K, Komiyama T, Miyazawa S, Shen ZN, Furumatsu T, Doi H, et al. Histone deacetylase inhibitor suppression of autoantibody-mediated arthritis in mice via regulation of p16INK4a and p21(WAF1/Cip1) expression. Arthritis Rheum. 2004;50(10):3365–76.
22. Young DA, Lakey RL, Pennington CJ, Jones D, Kevorkian L, Edwards DR, et al. Histone deacetylase inhibitors modulate metalloproteinase gene expression in chondrocytes and block cartilage resorption. Arthritis Res Ther. 2005;7(3):R503–12.
23. Chabane N, Zayed N, Afif H, Mfuna-Endam L, Benderdour M, Boileau C, et al. Histone deacetylase inhibitors suppress interleukin-1beta-induced nitric oxide and prostaglandin E2 production in human chondrocytes. Osteoarthr Cartil. 2008;16(10):1267–74.
24. Thomas CM, Fuller CJ, Whittles CE, Sharif M. Chondrocyte death by apoptosis is associated with cartilage matrix degradation. Osteoarthr Cartil. 2007;15(1):27–34.
25. Blanco FJ, Ochs RL, Schwarz H, Lotz M. Chondrocyte apoptosis induced by nitric oxide. Am J Pathol. 1995;146(1):75–85.
26. Otsuki S, Taniguchi N, Grogan SP, D'Lima D, Kinoshita M, Lotz M. Expression of novel extracellular sulfatases Sulf-1 and Sulf-2 in normal and osteoarthritic articular cartilage. Arthritis Res Ther. 2008;10(3):R61.
27. Guilak F, Alexopoulos LG, Upton ML, Youn I, Choi JB, Cao L, et al. The pericellular matrix as a transducer of biomechanical and biochemical signals in articular cartilage. Ann N Y Acad Sci. 2006;1068:498–512.
28. Jenuwein T, Allis CD. Translating the histone code. Science. 2001;293(5532):1074–80.
29. Urnov FD. Chromatin remodeling as a guide to transcriptional regulatory networks in mammals. J Cell Biochem. 2003;88(4):684–94.
30. Kruh J. Effects of sodium butyrate, a new pharmacological agent, on cells in culture. Mol Cell Biochem. 1982;42(2):65–82.
31. Chang S, Pikaard CS. Transcript profiling in Arabidopsis reveals complex responses to global inhibition of DNA methylation and histone deacetylation. J Biol Chem. 2005;280(1):796–804.
32. Reid G, Metivier R, Lin CY, Denger S, Ibberson D, Ivacevic T, et al. Multiple mechanisms induce transcriptional silencing of a subset of genes, including oestrogen receptor alpha, in response to deacetylase inhibition by valproic acid and trichostatin A. Oncogene. 2005;24(31):4894–907.
33. Nawaz Z, Baniahmad C, Burris TP, Stillman DJ, O'Malley BW, Tsai MJ. The yeast SIN3 gene product negatively regulates the activity of the human progesterone receptor and positively regulates the activities of GAL4 and the HAP1 activator. Mol Gen Genet. 1994;245(6):724–33.
34. Mariadason JM, Corner GA, Augenlicht LH. Genetic reprogramming in pathways of colonic cell maturation induced by short chain fatty acids: comparison with trichostatin A, sulindac,

and curcumin and implications for chemoprevention of colon cancer. Cancer Res. 2000;60(16):4561–72.
35. Chambers AE, Banerjee S, Chaplin T, Dunne J, Debernardi S, Joel SP, et al. Histone acetylation-mediated regulation of genes in leukaemic cells. Eur J Cancer. 2003;39(8):1165–75.
36. Libby P, Aikawa M. New insights into plaque stabilisation by lipid lowering. Drugs. 1998;56(suppl 1):9–13. (discussion 33).
37. McCawley LJ, Matrisian LM. Matrix metalloproteinases: multifunctional contributors to tumor progression. Mol Med Today. 2000;6(4):149–56.
38. Mitchell PG, Magna HA, Reeves LM, Lopresti-Morrow LL, Yocum SA, Rosner PJ, et al. Cloning, expression, and type II collagenolytic activity of matrix metalloproteinase-13 from human osteoarthritic cartilage. J Clin Invest. 1996;97(3):761–8.
39. Verdin E, Dequiedt F, Kasler HG. Class II histone deacetylases: versatile regulators. Trends Genet. 2003;19(5):286–93.
40. Chang S, Young BD, Li S, Qi X, Richardson JA, Olson EN. Histone deacetylase 7 maintains vascular integrity by repressing matrix metalloproteinase 10. Cell. 2006;126(2):321–34.
41. Jensen ED, Schroeder TM, Bailey J, Gopalakrishnan R, Westendorf JJ. Histone deacetylase 7 associates with Runx2 and represses its activity during osteoblast maturation in a deacetylation-independent manner. J Bone Miner Res. 2008;23(3):361–72.
42. Mengshol JA, Vincenti MP, Brinckerhoff CE. IL-1 induces collagenase-3 (MMP-13) promoter activity in stably transfected chondrocytic cells: requirement for Runx-2 and activation by p38 MAPK and JNK pathways. Nucleic Acids Res. 2001;29(21):4361–72.
43. Wang X, Manner PA, Horner A, Shum L, Tuan RS, Nuckolls GH. Regulation of MMP-13 expression by RUNX2 and FGF2 in osteoarthritic cartilage. Osteoarthr Cartil. 2004;12(12):963–73.
44. Kawaguchi H. Endochondral ossification signals in cartilage degradation during osteoarthritis progression in experimental mouse models. Mol Cells. 2008;25(1):1–6.
45. Kamekura S, Kawasaki Y, Hoshi K, Shimoaka T, Chikuda H, Maruyama Z, et al. Contribution of runt-related transcription factor 2 to the pathogenesis of osteoarthritis in mice after induction of knee joint instability. Arthritis Rheum. 2006;54(8):2462–70.
46. Venter JC, Adams MD, Myers EW, Li PW, Mural RJ, Sutton GG, et al. The sequence of the human genome. Science. 2001;291(5507):1304–51.
47. Iliopoulos D, Malizos KN, Tsezou A. Epigenetic regulation of leptin affects MMP-13 expression in osteoarthritic chondrocytes: possible molecular target for osteoarthritis therapeutic intervention. Ann Rheum Dis. 2007;66(12):1616–21.
48. Yun K, Im SH. Transcriptional regulation of MMP13 by Lef1 in chondrocytes. Biochem Biophys Res Commun. 2007;364(4):b1009–14.
49. Mengshol JA, Vincenti MP, Coon CI, Barchowsky A, Brinckerhoff CE. Interleukin-1 induction of collagenase 3 (matrix metalloproteinase 13) gene expression in chondrocytes requires p38, c-Jun N-terminal kinase, and nuclear factor kappaB: differential regulation of collagenase 1 and collagenase 3. Arthritis Rheum. 2000;43(4):801–11.
50. Brenner DA, O'Hara M, Angel P, Chojkier M, Karin M. Prolonged activation of jun and collagenase genes by tumour necrosis factor-alpha. Nature. 1989;337(6208):661–3.
51. Conca W, Kaplan PB, Krane SM. Increases in levels of procollagenase messenger RNA in cultured fibroblasts induced by human recombinant interleukin 1 beta or serum follow c-jun expression and are dependent on new protein synthesis. J Clin Invest. 1989;83(5):1753–7.
52. Borden P, Solymar D, Sucharczuk A, Lindman B, Cannon P, Heller RA. Cytokine control of interstitial collagenase and collagenase-3 gene expression in human chondrocytes. J Biol Chem. 1996;271(38):23577–81.
53. Baker AH, Edwards DR, Murphy G. Metalloproteinase inhibitors: biological actions and therapeutic opportunities. J Cell Sci. 2002;115(Pt 19):3719–27.

Downloaded from genesdev.cshlp.org on June 8, 2010 - Published by Cold Spring Harbor Laboratory Press

MicroRNA-140 plays dual roles in both cartilage development and homeostasis

Shigeru Miyaki, Tempei Sato, Atsushi Inoue, et al.

Genes Dev. 2010 24: 1173-1185 originally published online May 13, 2010
Access the most recent version at doi:10.1101/gad.1915510

Supplemental Material	**http://genesdev.cshlp.org/content/suppl/2010/05/03/gad.1915510.DC1.html**
References	This article cites 40 articles, 11 of which can be accessed free at: **http://genesdev.cshlp.org/content/24/11/1173.full.html#ref-list-1**
Related Content	**MicroRNA-140 and the silencing of osteoarthritis** Elisa Araldi and Ernestina Schipani Genes Dev. June 1, 2010 24: 1075-1080
Email alerting service	Receive free email alerts when new articles cite this article - sign up in the box at the top right corner of the article or **click here**

To subscribe to *Genes & Development* go to:
http://genesdev.cshlp.org/subscriptions

Copyright © 2010 by Cold Spring Harbor Laboratory Press

Downloaded from genesdev.cshlp.org on June 8, 2010 - Published by Cold Spring Harbor Laboratory Press

MicroRNA-140 plays dual roles in both cartilage development and homeostasis

Shigeru Miyaki,[1,4] Tempei Sato,[2,4] Atsushi Inoue,[2] Shuhei Otsuki,[1] Yoshiaki Ito,[2] Shigetoshi Yokoyama,[2] Yoshio Kato,[3] Fuko Takemoto,[2] Tomoyuki Nakasa,[2] Satoshi Yamashita,[2] Shuji Takada,[2] Martin K. Lotz,[1] Hiroe Ueno-Kudo,[2] and Hiroshi Asahara[1,2,5]

[1]Department of Molecular and Experimental Medicine, The Scripps Research Institute, La Jolla, California 92037, USA; [2]Department of Systems Biomedicine, National Research Institute for Child Health and Development, Tokyo 157-8535, Japan; [3]Biomedical Research Institute for Cell Engineering (RICE), National Institute of Advanced Industrial Science and Technology (AIST), Tsukuba 305-8562, Japan

Osteoarthritis (OA), the most prevalent aging-related joint disease, is characterized by insufficient extracellular matrix synthesis and articular cartilage degradation, mediated by several proteinases, including Adamts-5. miR-140 is one of a very limited number of noncoding microRNAs (miRNAs) specifically expressed in cartilage; however, its role in development and/or tissue maintenance is largely uncharacterized. To examine miR-140 function in tissue development and homeostasis, we generated a mouse line through a targeted deletion of miR-140. miR-140$^{-/-}$ mice manifested a mild skeletal phenotype with a short stature, although the structure of the articular joint cartilage appeared grossly normal in 1-mo-old miR-140$^{-/-}$ mice. Interestingly, miR-140$^{-/-}$ mice showed age-related OA-like changes characterized by proteoglycan loss and fibrillation of articular cartilage. Conversely, transgenic (TG) mice overexpressing miR-140 in cartilage were resistant to antigen-induced arthritis. OA-like changes in miR-140-deficient mice can be attributed, in part, to elevated *Adamts-5* expression, regulated directly by miR-140. We show that miR-140 regulates cartilage development and homeostasis, and its loss contributes to the development of age-related OA-like changes.

[*Keywords*: MicroRNA; miR-140; osteoarthritis; cartilage; *Adamts-5*]

Supplemental material is available at http://www.genesdev.org.

Received February 10, 2010; revised version accepted April 13, 2010.

MicroRNAs (miRNAs) are a class of noncoding RNAs that negatively regulate genes involved in numerous biological processes. Hundreds of miRNAs have been identified in various organisms, and many are evolutionarily conserved. Moreover, an estimated one-third of all mammalian mRNAs are regulated by miRNAs, demonstrating the essential role of miRNAs in controlling gene expression (Lewis et al. 2005). miRNAs are generated as long primary transcripts (pri-miRNAs) that are processed by the enzymes Drosha and Dicer into short ribonucleotides (~22 nucleotides long). The mature miRNAs are then incorporated into the RNA-induced silencing complex (RISC). The miRNA–RISC complex mediates the degradation of specific mRNA targets and/or the repression of mRNA translation via interactions with the 3′ untranslated regions (UTRs) that are partially sequence-specific (Bartel 2004). Several miRNAs exhibit a tissue-specific or developmental stage-specific expression pattern and have been associated with human diseases such as heart disease (van Rooij et al. 2006) and arthritis (Iliopoulos et al. 2008; Nakasa et al. 2008; Stanczyk et al. 2008; Yamasaki et al. 2009). In addition, mice with limb- or cartilage-specific deletion of the miRNA-processing enzyme Dicer exhibited a severe phenotype with reduced limb size but normal patterning (Harfe et al. 2005; Kobayashi et al. 2008). Dicer is indispensable for mature, functional miRNAs; therefore, this finding suggests that miRNAs play a critical role in skeletal development.

Recent studies have revealed the cartilage-specific expression of miR-140 in mouse embryos and zebrafish (Wienholds et al. 2005; Tuddenham et al. 2006). Using an miRNA microarray, we demonstrated considerable miRNA expression differences between human articular chondrocytes and mesenchymal stem cells. Furthermore, miR-140 exhibited the largest expression difference between the two cell types (Miyaki et al. 2009). The study of miR-140 may thus be the key miRNA to open a new insight of cartilage biology. However, the function of miRNAs in articular cartilage has not been analyzed by targeted deletion.

Previous studies also found reduced miR-140 expression in human osteoarthritis (OA) cartilage (Iliopoulos

[4]These authors contributed equally to this work.
[5]Corresponding author.
E-MAIL asahara@scripps.edu; FAX (858) 784-2695.
Article published online ahead of print. Article and publication date are online at http://www.genesdev.org/cgi/doi/10.1101/gad.1915510.

Downloaded from genesdev.cshlp.org on June 8, 2010 - Published by Cold Spring Harbor Laboratory Press

et al. 2008; Miyaki et al. 2009), which may contribute to the abnormal gene expression pattern characteristic of OA. These findings prompted us to examine the role of miR-140 in cartilage development and homeostasis by generating miR-140-deficient mice and cartilage-specific miR-140 transgenic (TG) mice. The results indicate that miR-140 plays dual roles in both cartilage development and homeostasis, in part via regulating *Adamts-5*, a major cartilage matrix-degrading protease in OA (Glasson et al. 2005; Stanton et al. 2005).

Results

Targeted deletion of cartilage-specific miR-140

To define the in vivo function of miR-140, we targeted the mouse miR-140 sequence for deletion. We deleted the region containing miR-140 in the intron between exons 16 and 17 of the WW domain-containing E3 ubiquitin protein ligase 2 (Wwp2), and inserted a neomycin (neo) resistance cassette flanked by loxP sites (Fig. 1A,B). The floxed phosphoglycerine kinase (PGK)-neo cassette was removed by crossing with Meox-Cre TG mice, and Cre-mediated neo excision was confirmed by genomic PCR (Fig. 1C). Quantitative real-time PCR (qPCR) analysis of chondrocyte RNA showed a complete absence of miR-140 in miR-140$^{-/-}$ mice (Fig. 1D). We confirmed that the Wwp2 protein levels were unchanged in miR-140$^{-/-}$ mice (Fig. 1E).

Skeletal growth in miR-140$^{-/-}$ mice

miR-140$^{-/-}$ mice were born in normal Mendelian ratios and were fertile. Skeletal development during embryogenesis in miR-140$^{-/-}$ mice appeared grossly normal (Fig. 2A). Postnatally, miR-140$^{-/-}$ mice manifested a mild skeletal phenotype, with short stature and low body weight (Fig. 2B–D), as well as craniofacial deformities characterized by a short snout and domed skull (Fig. 2E). This craniofacial phenotype in miR-140$^{-/-}$ mice shows partial similarity to that of cartilage-specific Dicer-deficient mice (Kobayashi et al. 2008), supporting the notion that miR-140 is a tissue-specific miRNA important in cartilage development. As miR-140 is expressed in cartilage and not in other tissues by whole-mount in situ hybridization (Wienholds et al. 2005; Tuddenham et al. 2006), reduced skeletal tissues of miR-140$^{-/-}$ mice may account for this weight loss phenotype.

The hind-limb bones were shorter in miR-140$^{-/-}$ mice compared with wild-type mice (Fig. 3A). In the growth plates of wild-type mice, miR-140 was expressed in proliferating chondrocytes but not in hypertrophic chondrocytes that expressed *Col10a1* (Fig. 3B). The width of the tibial growth plates in 1-mo-old mice was reduced in miR-140$^{-/-}$ mice compared with wild-type mice (Fig. 3C). The number of proliferating chondrocytes was significantly decreased at postnatal day 10 (P10) in miR-140$^{-/-}$ mouse growth plates (Fig. 3D,E), whereas no significant changes were observed in hypertorophyic zones (Fig. 3C). These findings indicate that the mild skeletal phenotype in miR-140$^{-/-}$ mice with short stature results from a reduction in proliferating chondrocytes.

OA-like pathology in miR-140$^{-/-}$ mouse knee joints

Chondrocytes play a critical role not only in skeletal development, but also in articular cartilage formation and maintenance. Analysis of pri-miR-140 expression in 2-mo-old wild-type mice by in situ hybridization showed miR-140 expression in chondrocytes from the surface to middle zones of articular cartilage and in the menisci, overlapping with expression of the chondrocyte marker *Col2a1* (Fig. 4A). Furthermore, the structure and shape of knee joints—including articular cartilage, menisci, and ligaments—were analyzed by Safranin O staining and three-dimensional (3D) computed tomography (CT). They all appeared to be normal in miR-140$^{-/-}$ mice at birth and 1 mo of age (Supplemental Fig. S1).

Because miR-140 expression was shown to be reduced in human OA cartilage (Iliopoulos et al. 2008; Miyaki et al. 2009), we examined the potential role of miR-140 in cartilage homeostasis. OA initiation and progression is mediated by various stimuli and circumstances, including the following three main factors: age-related changes in homeostatic balance, excessive mechanical stress sometimes triggered by joint injury, and transient inflammation in the articular joint damaging the cartilage matrix. Therefore, to determine the potential role of miR-140 in cartilage homeostasis, we used three different animal models of OA: an aging model, a surgical model, and an antigen-induced arthritis (AIA) model.

First, we tested whether loss of miR-140 affected age-related onset of OA changes, and observed that miR-140$^{-/-}$ mice developed an age-related OA-like pathology. Knee joints from 3-mo-old mice showed reduced Safranin O staining in femoral condyles and tibial plateaus, indicative of proteoglycan loss (Fig. 4B). By 8 mo, overt cartilage degradation was apparent as more severe proteoglycan loss, a roughened articular surface, and fibrillation; these changes were not observed in age-matched wild-type mice (Fig. 4B). By 12 mo, miR-140$^{-/-}$ mice showed severe structural cartilage defects (Fig. 4B) that were not associated with synovial hyperplasia. We also observed OA-like changes in elbow and ankle joint articular cartilage of miR-140$^{-/-}$ mice at 12 mo old, compared with articular cartilage from wild-type mice (Supplemental Fig. S2). To quantify OA-like pathological changes in the articular cartilage, an OA scoring system was used to validate several aspects of the histological changes (Chambers et al. 2001; Glasson et al. 2004). OA scores were significantly higher in miR-140$^{-/-}$ mice compared with wild-type mice (Fig. 4C). These results support the hypothesis that miR-140 is a critical regulator of cartilage homeostasis, and its loss contributes to cartilage degradation characteristic of OA.

Next, we used the surgical arthritis model, in which the articular cartilage was exposed to an excessive mechanical load, due to joint instability caused by surgical resection of the medial meniscotibial ligament (MMTL) (Glasson et al. 2007). Consistent with observations in the aging OA model, the surgical arthritis model also demonstrated

Downloaded from genesdev.cshlp.org on June 8, 2010 - Published by Cold Spring Harbor Laboratory Press

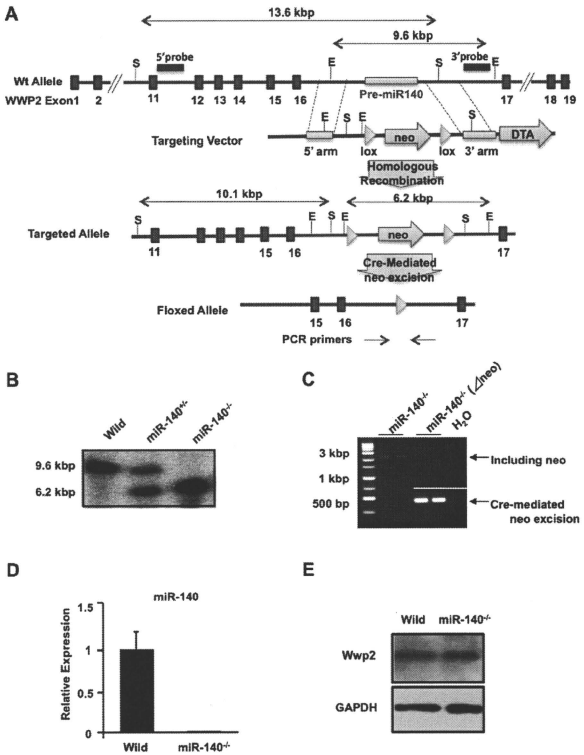

Figure 1. Generation of miR-140-null mice. (*A*) Targeting of miR-140. The targeting vector was constructed to replace the endogenous pri-miR-140 locus with a PGK-neo cassette by homologous recombination. The 5′ probe and 3′ probe used for Southern blot and PCR primers used for genotyping are indicated. (E) EcoRV, (S) SphI. (*B*) Southern blot analysis of wild-type (Wild) and miR-140 mutant mice. Genomic DNA was digested with EcoRV and probed with the indicated 3′ probe. (*C*) Confirmation of Cre-mediated neo excision by genomic PCR. The floxed PGK-neo cassette was removed by crossing with Meox-Cre TG mice. (*D*) Expression of mature miR-140 in wild-type (Wild) and miR-140$^{-/-}$ mouse embryos at E11.5 as assessed by qPCR. Mature miR-140 was not detected in miR-140$^{-/-}$ mice. Data are expressed as mean ± SEM ($n = 3$). (*E*) Western blot analysis of Wwp2. Wwp2 expression was not detectably different in miR-140$^{-/-}$ compared with wild-type mice.

that miR-140$^{-/-}$ mice exhibit accelerated proteoglycan loss and fibrillation of articular cartilage in knee joints compared with the wild-type mice at 8 wk after surgery, which is reflected in higher OA scores (Fig. 4D,E).

Cartilage-specific miR-140 TG mice exhibited resistance to AIA

We further examined the role of miR-140 in articular cartilage by using the AIA model, in which transient inflammation was induced by antigen injection. Inflammatory signals such as interleukin-1β (IL-1β) from the chondrocytes and synovial membrane of articular joint spaces mediate OA progression, in part by up-regulating the expression of cartilage matrix degradation enzymes in chondrocytes (Goldring and Goldring 2007). In this model, as well as in human OA pathogenesis, transient joint inflammation causes cartilage damage by the induction of cartilage-degrading enzymes. The AIA model is advantageous in that it leads to cartilage damage in a

Downloaded from genesdev.cshlp.org on June 8, 2010 - Published by Cold Spring Harbor Laboratory Press

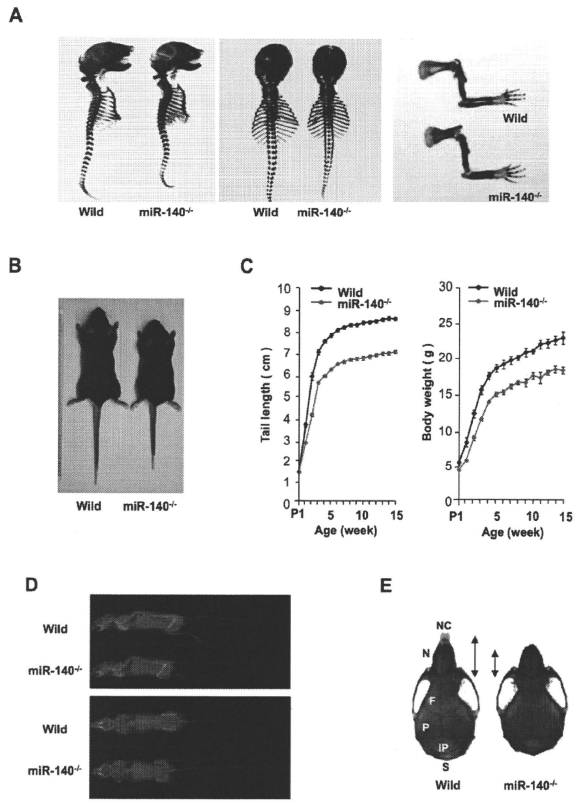

Figure 2. Growth retardation in *miR-140*$^{-/-}$ mice. (*A*) Skeletal preparation with Alcian blue/Alizarin red staining of wild-type (Wild) and miR-140$^{-/-}$ littermates at E17.5. miR-140$^{-/-}$ embryos exhibited no overt abnormalities in skeletal development. (*Left*) Whole-mount.(*Middle*) Dorsal view. (*Right*) Forelimb. (*B*) Appearance of wild-type and miR-140$^{-/-}$ mice at 4 wk. Growth retardation was observed in miR-140$^{-/-}$ mice. (*C*) Wild-type and miR-140$^{-/-}$ mice were scored for tail length and body weight at various postnatal stages. miR-140$^{-/-}$ mice showed growth retardation 1 wk after birth (tail length, $P < 0.01$; body weight, $P < 0.05$). Data are expressed as mean ± SEM (n = 5–12). (*D*) No gross skeletal changes were detectable by X-ray in 3-mo-old mice. (*E*) Skulls of wild-type and miR-140$^{-/-}$ mice stained with Alcian blue/Alizarin red. Dorsal views are shown. miR-140$^{-/-}$ mice exhibited craniofacial bone defects characterized by short nasal bone, short maxilla, and domed skull. (NC) Nasal capsule, (N) nasal bone, (F) frontal bone, (P) parietal bone, (IP) interparietal bone, (S) supraoccipital bone.

short time in wild-type mice, which enables us to monitor the beneficial effects of miR-140 against cartilage degradation by a gain-of-function approach.

Accordingly, we generated cartilage-specific TG mice in which miR-140 expression was driven by a well-characterized *Col2a1* enhancer sequence (Fig. 5A; Zhou et al. 1995; Krebsbach et al. 1996). We obtained three lines of TG mice and observed up-regulation of miR-140 in cartilage of all three lines (Fig. 5B). These TG mice did not show any apparent abnormalities in skeletal development (data

Downloaded from genesdev.cshlp.org on June 8, 2010 - Published by Cold Spring Harbor Laboratory Press

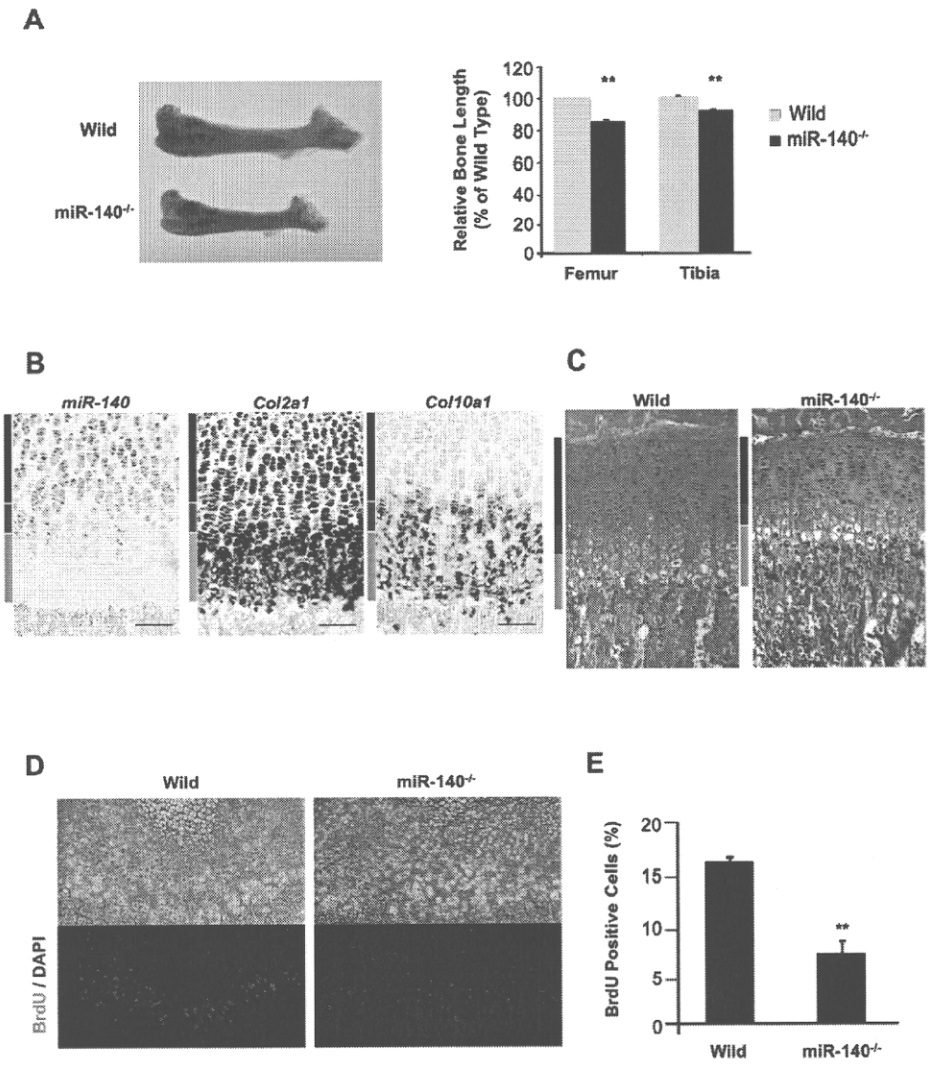

Figure 3. Skeletal growth in miR-140$^{-/-}$ mice. (*A*, *left*) Length of femur. (*Right*) Long bones were significantly shorter in the miR-140$^{-/-}$ mice. Data are expressed as mean ± SEM ($n = 3$). (**) $P < 0.01$. (*B*) Expression of *pri-miR-140*, *Col2a1*, and *Col10a1* in the tibial growth plates of P10 mice. miR-140 was detected in proliferating chondrocytes. (Blue bar) Proliferative zone, (red bar) prehypertrophic zone, (green bar) hypertrophic zone. (*C*) Safranin O staining of the tibial growth plates in 1-mo-old mice. The proliferating zone was reduced in miR-140$^{-/-}$ mice compared with wild-type mice (Wild). (*D*,*E*) BrdU-positive cells were significantly reduced in miR-140$^{-/-}$ mice at P10. BrdU (green) and DAPI (blue) staining indicate nuclei. Data are expressed as mean ± SEM ($n = 3$). (**) $P < 0.01$.

not shown). To examine whether the miR-140 level in articular chondrocytes affects cartilage sensitivity to experimental challenge, we assessed AIA in knee joints of miR-140 TG mice, miR-140$^{-/-}$ mice, and wild-type mice. We observed similar levels of synovial hyperplasia among miR-140 TG mice, miR-140$^{-/-}$ mice, and wild-type mice; however, miR-140$^{-/-}$ mice showed reduced Safranin O staining (Fig. 5C). Importantly, miR-140 TG mice were resistant to proteoglycan and type II collagen loss compared with wild-type mice. To quantify the extent of matrix degradation, we used the Mankin scoring system (Mankin 1971; Zemmyo et al. 2003) for proteoglycan loss. Mankin scores were significantly lower in miR-140 TG mice and significantly higher in miR-140$^{-/-}$ mice compared with wild-type mice (Fig. 5D). These findings are consistent with the idea that miR-140 protects against OA progression.

ADAMTS-5 is a direct target of miR-140 and mediates OA pathogenesis

Identification of miR-140 target genes can provide new insights into miR-140 function and OA pathogenesis. To achieve this goal, we applied DNA array analysis to identify miRNA targets (Lim et al. 2005; Valencia-Sanchez et al. 2006). Based on computationally predicted target

Downloaded from genesdev.cshlp.org on June 8, 2010 - Published by Cold Spring Harbor Laboratory Press

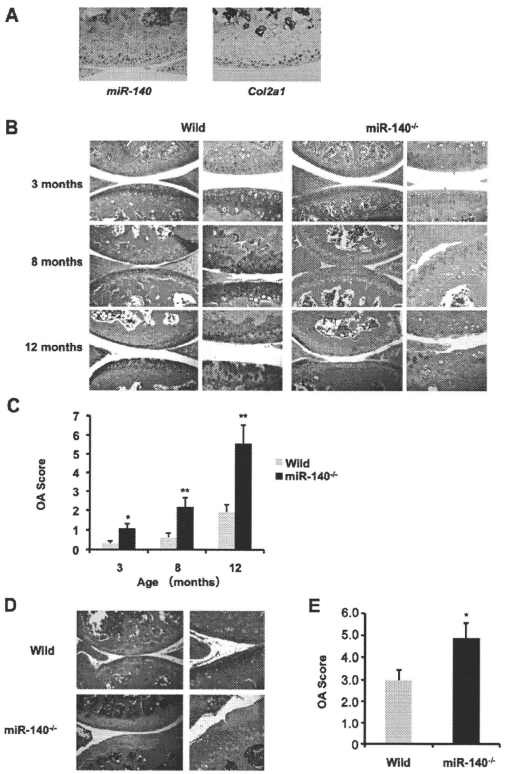

Figure 4. miR-140$^{-/-}$ mice exhibit OA-like pathology. (*A*) Expression of *pri-miR-140* (*left*) and *Col2a1* (*right*) in articular cartilage of the knee joints in 2-mo-old mice. miR-140 was detected in chondrocytes from the surface to middle zones of articular cartilage. (*B*) Safranin O staining of the knee joint in 3-mo-old mice (wild-type, $n = 6$; miR-140$^{-/-}$, $n = 6$), 8-mo-old mice (wild-type, $n = 15$; miR-140$^{-/-}$, $n = 13$), and 12-mo-old mice (wild-type, $n = 12$; miR-140$^{-/-}$, $n = 11$). miR-140 deletion caused an early onset of OA-like changes. (*C*) Histopathologic scores of knee joints. OA scores were significantly increased in miR-140$^{-/-}$ mice. Data are expressed as mean ± SEM. (*) $P < 0.05$; (**) $P < 0.01$. (*D*) Surgical OA was induced in 10-wk-old wild-type and miR-140$^{-/-}$ mice by resecting the MMTL (wild-type mice, $n = 8$; miR-140$^{-/-}$ mice, $n = 11$). The knee joints were harvested 8 wk after surgery and stained with Safranin O for histopathologic analysis. (*E*) miR-140$^{-/-}$ mice showed significantly increased OA scores compared with wild-type mice after surgery. Data are expressed as mean ± SEM. (*) $P < 0.05$.

genes found in the online database TargetScan (http://www.targetscan.org), 17 of the mRNAs in the array that were increased in miR-140$^{-/-}$ chondrocytes exhibited conserved miR-140-binding sites in their 3′ UTRs with 7-mer or 8-mer seeds (Supplemental Table S1). Among the most overexpressed was the gene for ADAMTS-5, which degrades aggrecan and is a critical enzyme for OA pathogenesis (Glasson et al. 2005; Stanton et al. 2005). We analyzed *Adamts-5* sequences in humans, mice, rats, and dogs and observed highly conserved miR-140-binding sites with 8-mer seeds in the *Adamts-5* 3′ UTR (Fig. 6A). *Adamts-5* expression was significantly increased in chondrocytes from miR-140$^{-/-}$ mice and significantly decreased in those from miR-140 TG mice compared with wild-type (Fig. 6B). Similarly, increased ADAMTS-5 protein expression in articular cartilage in miR-140$^{-/-}$ mice at 1 and 3 mo old was visualized by immunohistochemistry (Fig. 6C,D; Supplemental Fig. S3). To confirm that miR-140 plays a critical role in aggrecanolysis, we quantified proteoglycan loss from cartilage in wild-type mice, miR-140 TG mice, and miR-140$^{-/-}$ mice. Femoral head cartilage explants were cultured with or without IL-1β, which is a potent catabolic stimulus of cartilage matrix degradation. Cartilage explants from miR-140$^{-/-}$ mice showed significantly increased proteoglycan release compared with wild-type cartilage (Fig. 6E). In contrast, IL-1β-induced proteoglycan release from the cartilage of miR-140 TG mice was significantly lower compared with wild-type cartilage.

We further tested whether miR-140 regulates *Adamts-5* mRNA in chondrocytes. Treatment of chondrocytes from

Downloaded from genesdev.cshlp.org on June 8, 2010 - Published by Cold Spring Harbor Laboratory Press

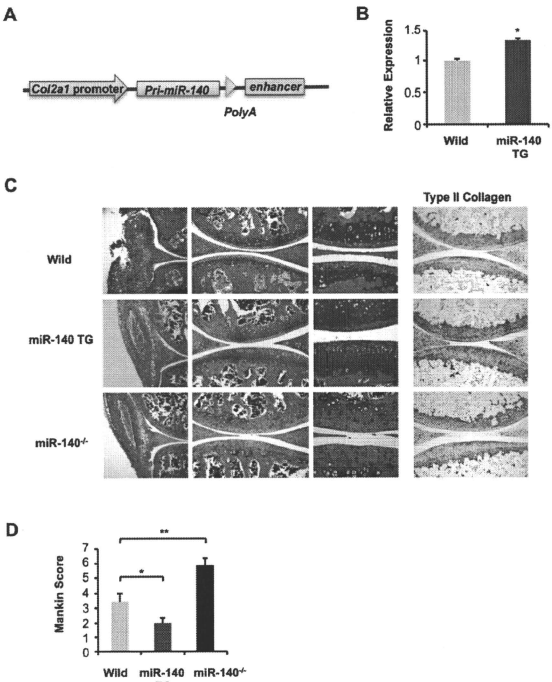

Figure 5. Cartilage-specific miR-140 TG mice are resistant to AIA. (*A*) miR-140 TG mice were generated with a construct using the cartilage-specific *Col2a1* promoter. (*B*) Significantly increased expression of miR-140 in chondrocytes of miR-140 TG mice compared with those of wild-type mice was confirmed by qPCR analysis. These data are results from representatives of a single mouse line ($n = 3$). Data are expressed as mean ± SEM. (*) $P < 0.05$. (*C*) Seven days after induction of AIA, Safranin O staining and immunohistochemistry for type II collagen shows higher proteoglycan and collagen levels in miR-140 TG mice and lower levels in miR-140$^{-/-}$ mice compared with wild type. (*D*) Mankin score for proteoglycan loss in wild-type mice ($n = 5$), miR-140 TG mice ($n = 6$), and miR-140$^{-/-}$ mice ($n = 6$) 7 d after induction of AIA. Data are expressed as mean ± SEM. (*) $P < 0.05$; (**) $P < 0.01$.

miR-140$^{-/-}$ mice with ds-miR-140 reduced *Adamts-5* expression (Fig. 6F), supporting the notion that miR-140 negatively regulates *Adamts-5* mRNA. To determine whether *Adamts-5* is a direct miR-140 target in intact cells, the Adamts-5 3′ UTR, which includes a putative miR-140-binding site, was cloned downstream from the luciferase gene in an expression vector driven by the SV-40 promoter (*Adamts-5* 3′ UTR). Cotransfection of HEK293T cells with ds-miR-140 significantly reduced luciferase activity in cells transfected with *Adamts-5* 3′ UTR (Fig. 6G). No changes in luciferase activity were observed in cells transfected with the mutated luciferase expression vector (*Adamts-5* mut 3′ UTR) in response to ds-miR-140 (Fig. 6G). Taken together, these data indicate that miR-140 directly regulates *Adamts-5* expression and proteoglycan loss in articular cartilage.

Discussion

Recent studies have revealed that miRNAs play critical roles in various biological events, including development, disease, and immunity (Stefani and Slack 2008; Xiao and Rajewsky 2009). However, few molecular networks regulated by miRNAs have been characterized in detail, due in part to difficulty in determining the direct targets of each miRNA. Tissue-specific miRNAs targeting mice have

Downloaded from genesdev.cshlp.org on June 8, 2010 - Published by Cold Spring Harbor Laboratory Press

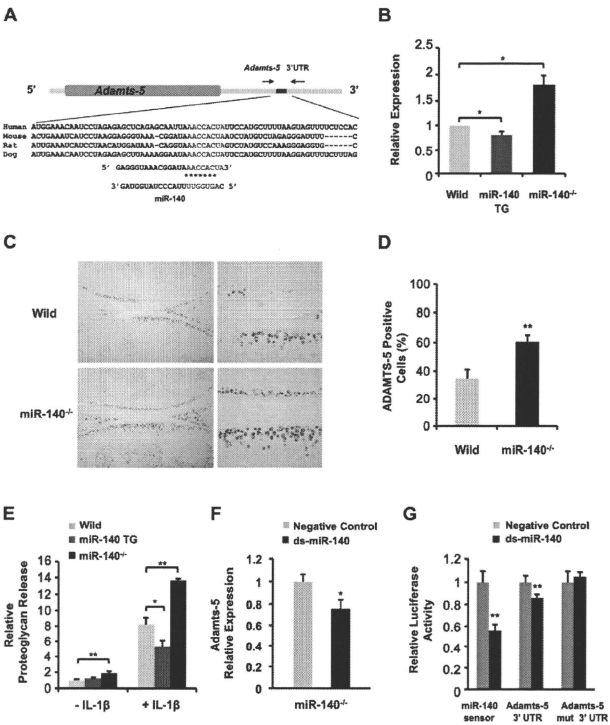

Figure 6. miR-140 regulates *Adamts-5* expression. (*A*) miR-140 targets the *Adamts-5* 3′ UTR. Sequence alignment of a putative miR-140-binding site in the *Adamts-5* 3′ UTR shows a high level of sequence conservation and complementarity with miR-140. (*B*) Differential *Adamts-5* expression in rib chondrocytes from wild-type mice, miR-140 TG mice, and miR-140$^{-/-}$ mice was evaluated by qPCR. Data are expressed as fold differences compared with wild-type chondrocytes (mean ± SEM; $n = 4$–5 per genotype). (*) $P < 0.05$. (*C*) Histologic analysis of articular cartilage from 3-mo-old mice. Immunostaining showed an increase in ADAMTS-5-positive chondrocytes in miR-140$^{-/-}$ mice. (*D*) ADAMTS-5-positive cells were detected in wild-type and miR-140$^{-/-}$ cartilage. Knee joints from 3-mo-old wild-type ($n = 3$) and miR-140$^{-/-}$ ($n = 3$) mice were examined. Data are expressed as mean ± SEM. (**) $P < 0.01$. (*E*) Femoral head cartilage explants from miR-140$^{-/-}$ mice cultured in DMEM only ($n = 13$) or DMEM containing IL-1β ($n = 6$) showed significantly increased proteoglycan release compared with wild-type mice in DMEM only ($n = 17$) or DMEM containing IL-1β ($n = 6$). IL-1β-induced proteoglycan release in miR-140 TG mice in medium ($n = 12$) was significantly lower compared with that of wild-type mice ($n = 10$). Data are expressed as fold differences compared with wild-type explants in DMEM only (mean ± SEM). (*) $P < 0.05$; (**) $P < 0.01$. (*F*) Relative *Adamts-5* expression in miR-140$^{-/-}$ chondrocytes was determined by qPCR after transfection with ds-miR-140 (black). Data are expressed as fold differences relative to negative control cells (gray, mean ± SEM). (*) $P < 0.05$. (*G*) Luciferase activity of pLuc2-miR-140 sensor (miR-140 sensor), pLuc2-*Adamts-5* 3′ UTR (*Adamts-5* 3′ UTR), and pLuc2-*Adamts-5* 3′ UTR with mutated miR-140-binding site (*Adamts-5* mut 3′ UTR). Luciferase activity was determined in HEK293T cells transfected with miR-140 sensor, *Adamts-5* 3′ UTR, or *Adamts-5* mut 3′ UTR along with a ds-miR-140 (black) or negative control miRNA (gray) ($n = 6$). Data are expressed as relative luciferase activity (mean ± SEM). (*) $P < 0.05$; (**) $P < 0.01$.

been generated to elucidate the role of miRNAs in tissue and organ development, including heart and muscles (van Rooij et al. 2007; Zhao et al. 2007; Liu et al. 2008); however, so far there is very limited information on the function of miRNAs in cartilage/bone development and related diseases.

Downloaded from genesdev.cshlp.org on June 8, 2010 - Published by Cold Spring Harbor Laboratory Press

Transcription factor SRY-box-containing gene 9 (Sox9) is a master regulator of chondrocyte differentiation (de Crombrugghe et al. 2000). The expression of miR-140 shadows *Sox9* expression, and the deletion of Sox9 diminishes miR-140 expression during embryogenesis (S Miyaki and H Asahara, unpubl.), indicating that miR-140 is under Sox9 regulation in chondrocytes. Although the disruption of Sox9 in mice results in a complete lack of cartilage development, miR-140$^{-/-}$ mice showed only a mild skeletal phenotype, with short stature and craniofacial changes. Results of studies targeting mice at specific developmental stages show that Sox9 is not only essential for chondrogenesis initiation, but is also important to produce large numbers of proliferating chondrocytes (Akiyama 2008). In the present study, the expression pattern of miR-140 was detected in the proliferation zone during endochondral ossification, and fewer proliferating chondrocytes were observed in miR-140$^{-/-}$ mice. Thus, regulation of proliferating chondrocytes may be one of the Sox9 functions mediated by miR-140.

Mice that are Dicer-deficient in cartilage tissues show a progressive and profound reduction in proliferating growth plate chondrocytes, which leads to severe skeletal growth defects and premature death (Kobayashi et al. 2008); however, this severe phenotype may reflect the effect of reducing all miRNAs, including ubiquitous ones. In this regard, our study provides the first example showing bone and cartilage phenotypes in mice caused by tissue-specific miRNA.

The phenotype of miR-140$^{-/-}$ mice on skeletal framework is not drastic, and the mice can survive for >1 yr; however, this mild phenotype provides us with an opportunity to monitor another aspect of miR-140 function in cartilage. Chondrocytes have two major functions: endochondral ossification for proper skeletal development, and articular cartilage maintenance for joint movement. Although chondrocytes in endochondral ossification disappear after bone development has been completed, articular cartilage chondrocytes persist, secreting the extracellular matrix that protects tissue from damage. The role of miRNAs in tissue homeostasis has not yet been well elucidated, other than a few studies such as those reporting the critical role of miR-143/145 in smooth muscle cell maintenance (Elia et al. 2009).

Articular cartilage is a good tissue for characterizing the molecular network involved in tissue homeostasis. The cartilage framework consists of a cartilage-specific extracellular matrix, which includes type II collagen and proteoglycans, and is maintained by chondrocytes embedded in the matrix. To maintain the integrity of this cartilage framework, the matrix is continuously undergoing remodeling via matrix-degrading enzymes; this degradation is balanced by the secretion of newly synthesized matrix proteins. The balance of these catabolic and anabolic signals in cartilage tissue is critical for cartilage homeostasis; aging, inflammation, or injuries may promote catabolic signals, including ADAMTS-5 and matrix metallopeptidase-13 (MMP-13), which can lead to arthritis changes. OA is the result of this age-related loss of the homeostatic balance between cartilage degradation and repair; it is aggravated by joint inflammation or excessive mechanical load (Goldring and Goldring 2007; Hashimoto et al. 2008; Goldring and Marcu 2009). Treatment options are limited, and new therapeutic targets that regulate the cartilage homeostasis balance should be sought.

To determine the role of miR-140 in articular cartilage, we examined three different arthritis models: age-related, surgical, and inflammatory (AIA). Disruption of miR-140 in vivo induced the early onset of spontaneous OA-like changes in articular cartilage of the age-related model and more severe OA-like changes in the surgical model. Transfection of human chondrocytes with ds-miR-140 down-regulated IL-1β-induced Adamts-5 expression (Miyaki et al. 2009). Consistent with our findings that miR-140 exerts a protective effect in cartilage, miR-140 TG mice were resistant to cartilage matrix degradation in the inflammatory model, suggesting that the regulation of miR-140 has important implications for drug design in OA treatment.

To address the mechanism of enhanced cartilage degradation in miR-140$^{-/-}$ mice, we showed the up-regulation of *Adamts-5*, a direct target of miR-140. ADAMTS-5 was shown to be a critical cartilage-degrading enzyme, because animals deficient in ADAMTS-5 activity are resistant to cartilage degeneration in the surgical OA model and inflammatory arthritis model (Glasson et al. 2005; Stanton et al. 2005). ADAMTS-5 also appears to be the major enzyme responsible for aggrecan degradation in human OA on the basis of increased mRNA and protein expression in OA cartilage (Malfait et al. 2002). Nevertheless, regulatory mechanisms of *Adamts-5* expression have not been clearly elucidated. Two groups reported recently that Runx2 regulates *Adamts-5* expression (Thirunavukkarasu et al. 2007), and hedgehog signaling regulates the expression of *Adamts-5* via Runx2 (Lin et al. 2009). In addition to these transcriptional regulations, in the present study we demonstrated that *Adamts-5* expression was tightly regulated by miR-140 at the post-transcriptional level.

Although the critical role of miR-140 in cartilage maintenance may be explained largely by identifying *Adamts-5* as its direct target, miRNAs are believed to regulate multiple target mRNAs; therefore, the role of miR-140 in cartilage homeostasis may involve the regulation of additional genes, as listed in Supplemental Table S1. Accordingly, gene expression analysis by microarray and qPCR revealed an up-regulation of other cartilage-related catabolic factors, such as matrix degradation enzymes, and a down-regulation of cartilage matrix genes in chondrocytes of miR-140$^{-/-}$ mice as early as P3 (Supplemental Fig. S2). These results suggest that miR-140 may suppress pathways other than *Adamts-5* expression, thus regulating the overall balance of cartilage matrix synthesis and degradation. Histone deacetylase 4 (HDAC4), which inhibits hypertrophic differentiation of chondrocytes (Vega et al. 2004), is thought to be an miR-140 target gene (Tuddenham et al. 2006); however, we did not observe significant changes in HDAC4 mRNA or protein expression in the endochondral plate or articular cartilage in the present study. The miR-140$^{-/-}$ and miR-140 TG lines may be useful in identifying other targets associated with cartilage development and homeostasis.

Downloaded from genesdev.cshlp.org on June 8, 2010 - Published by Cold Spring Harbor Laboratory Press

Taken together, our findings demonstrate that miR-140 is required for skeletal development and cartilage homeostasis, and protects against OA-like pathology via *Adamts-5* regulation (Fig. 7). We conclude that miR-140 is a novel regulator of cartilage homeostasis, and changes in its expression and function play an important role in diseases associated with cartilage destruction, including OA and inflammatory arthropathies.

Materials and methods

Generation of miR-140-null mice and miR-140 TG mice

All animal experiments were performed according to protocols approved by the Institutional Animal Care and Use Committee at The Scripps Research Institute and National Institute for Child Health and Development. A vector was constructed to replace the endogenous miR-140 locus with a PGK-neo cassette by homologous recombination in embryonic stem (ES) cells. The 5′ and 3′ sequences flanking the endogenous miR-140 locus were amplified by PCR from a C57BL/6 genomic BAC clone (BACPAC Resource Center). These homologous arms were cloned into a vector incorporating both a neomycin resistance cassette for positive selection and a diphtheria toxin (DTA) gene for negative selection. The targeting vector was linearized and electroporated into TT2F mouse ES cells. Recombinant ES clones were isolated after culture in medium containing G418 antibiotic. Clones were then screened for proper integration by Southern blot analysis with the 5′ probe, 3′ probe, and neomycin resistance cassette sequence indicated in Figure 1. After proper integration was validated by genomic sequencing, two clones were chosen for microinjection into eight-cell-stage embryos. The resulting chimeric offspring were crossed with C57BL/6 mice, and germline transmission was confirmed by Southern blot and PCR. The floxed PGK-neo cassette was removed by crossing with Meox-Cre TG mice; Cre-mediated neo excision was confirmed by genomic PCR.

To generate cartilage-specific miR-140 TG mice, a pri-miR-140 fragment was PCR-amplified from mouse chondrocyte cDNA with the primers 5′-TGGTGTGTGGTTCTATGCCAGC-3′ and 5′-AGCCTCAAGCCAGAATTCAGG-3′.

pri-miR-140 was cloned into the NotI site of a Col2a1-based expression vector (Ueta et al. 2001), which contained the promoter and enhancer of the mouse Col2a1 gene. TG mice were generated by pronuclear injection of the transgene into the B6 strain, and were backcrossed to a C57BL/6 background. Genomic DNA isolated from the tail was analyzed by PCR using specific primers or transgene probes (forward primer, 5′-CAGGCTGTGCTTGGTGGGCATCTG-3′; reverse primer, 5′-CTAGCCTAGGCTCGAGAAGCTTGCT-3′).

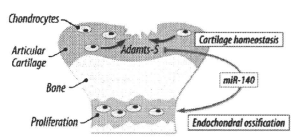

Figure 7. *Adamts-5* regulation via miR-140 is required for skeletal development and cartilage homeostasis. miR-140 has dual roles in both endochondral ossification and articular cartilage homeostasis. During endochondral ossification, miR-140 is important for chondrocyte proliferation, although its targets are unclear. miR-140 also plays a critical role in articular cartilage homeostasis by repressing *Adamts-5* expression.

qPCR

qPCR was performed using TaqMan Gene Expression Assay probes for *Adamts-5* (Mm01344182_m1) and glyceraldehyde 3-phosphate dehydrogenase (*GAPDH*; Mm 99999915_g1; Applied Biosystems), and qPCR for miR-140 was performed using the TaqMan MicroRNA Reverse Transcription kit (Applied Biosystems) according to the manufacturer's protocol. *GAPDH* or sno202 was used as an internal control to normalize sample differences.

Western blot analysis

Total protein extracts of wild-type and miR-140$^{-/-}$ chondrocytes were prepared for Western blot analysis. The Wwp2 protein, which is encoded by the host gene of miR-140, was detected by the AIP2 antibody (dilution, 1:2000; sc-11896, Santa Cruz Biotechnologies).

Radiologic imaging

X-ray and micro-CT imaging were performed using LaTheta LCT-200 (Aloka) according to the manufacturer's instructions. Three-dimensional CT images of the knee joint were recreated by using VGStudio MAX 2.0 software (Nihon Visual Science).

Bromodeoxyuridine (BrdU) labeling, RNA in situ hybridization, and immunohistochemistry

Proliferating cells were detected by BrdU incorporation using the In Situ Cell Proliferation kit, FLUOS (Roche); 4′,6-diamidino-2-phenylindole (DAPI) served as a counterstain. In situ hybridization of miR-140 was performed as described previously (Yokoyama et al. 2009). We used a probe specific for the primary region of miR-140. The sections of knee joints were immunostained using antibodies against ADAMTS-5 (ab13976, Abcam) and type II collagen (II-II6B3, Hybridoma Bank).

Histopathologic assessment

The miR-140$^{-/-}$ mice and wild-type littermates were obtained from the intercross of miR-140$^{+/-}$ maintained in a C57BL/6 background. Whole-mount Alcian blue and Alizarin red S staining of skeletons were performed on wild-type and miR-140$^{-/-}$ embryos at embryonic day 17.5 (E17.5). Mice were euthanized, and knee joints were harvested from 3-, 8-, and 12-mo-old mice. The knee joints were fixed in 10% zinc-buffered formalin (Z-Fix; Anatech) and decalcified in decalcifier (TBD-2; Shandon). For each animal, 4-μm sagittal sections through the central weight-bearing region of the medial femorotibial joint were stained with Safranin O and Fast Green for analysis of histopathologic differences between wild-type and miR-140$^{-/-}$ mice. The proteoglycan content of articular cartilage was scored using the previously reported Mankin scoring system (Mankin 1971; Zemmyo et al. 2003). OA scores indicating the severity of cartilage degeneration were evaluated for wild-type (n = 6) and miR-140$^{-/-}$ (n = 6) 3-mo-old mice, wild-type (n = 15) and miR-140$^{-/-}$ (n = 13) 8-mo-old mice, and wild-type (n = 12) and miR-140$^{-/-}$ (n = 11) 12-mo-old mice. At least four sections per sample were analyzed microscopically and scored using previously reported semiquantitative scoring systems (Chambers et al. 2001; Glasson et al. 2004).

Downloaded from genesdev.cshlp.org on June 8, 2010 - Published by Cold Spring Harbor Laboratory Press

Mouse model of surgically induced OA

Surgical OA was induced in wild-type and miR-140$^{-/-}$ mice at the age of 10 wk by resecting the MMTL in the right knee joint (Glasson et al. 2007). Pathological changes in medial tibial plateau and medial femoral condyle of the joint were evaluated after 8 wk on safranin-O-stained sections by OA score.

Mouse model of AIA

Inflammatory arthritis was induced in knee joints of 10-wk-old wild-type (n = 5), miR-140$^{-/-}$ (n = 6), and miR-140 TG (n = 6) mice by intra-articular injection of methylated bovine serum albumin (mBSA; Sigma catalog no. A1009) in mice preimmunized with mBSA. On day 1, mice were preimmunized by a 100-μL intradermal injection at the base of the tail with an emulsion containing 100 μg of mBSA (in 0.9% saline) and an equal volume of Freund's complete adjuvant (Sigma catalog no. F5881). On day 10, animals were treated with intra-articular mBSA (10 μL of 20 mg/mL mBSA in 0.9% sterile saline or vehicle alone) into the left and right knee joints. On day 17, the knee joints were harvested and processed using standard procedures.

DNA microarray analysis

DNA microarray analysis was performed using the Affymetrix mouse genome 430 2.0 array. RNA samples were collected from cultured rib chondrocytes of wild-type and miR-140$^{-/-}$ mice at P3. Microarray data were summarized by the Robust Multichip Average (RMA) method, and statistical analysis was performed using National Institute on Aging (NIA) Array Analysis (http://Igsun.grc.nia.nih.gov/ANOVA). The microarray data were deposited in the Gene Expression Omnibus (GEO) repository under accession number GSE16007.

Bioinformatics and miR-140 target analysis

We performed searches on the TargetScan prediction program (http://targetscan.org) for the predicted targets of miR-140.

Quantification of proteoglycan

Femoral heads were harvested from 4-wk-old wild-type and miR-140$^{-/-}$ mice. The explants were cultured for 3 d with or without IL-1β (5 ng/mL) in Dulbecco's modified Eagle's medium (DMEM) containing 10 mM HEPES and 1% penicillin/streptomycin. At the end of the culture, the cartilage explants were digested with protease K solution (Tris-EDTA at pH 8.0, 30 μg/mL protease K, 0.5% Tween 20) overnight at 50°C. Proteoglycan content in the protease K digests and conditioned medium were determined using the Blyscan Glycosaminoglycan Assay kit (Biocolor).

Cell culture and transfection of ds-miR-140 assay

Mouse chondrocytes were prepared from rib cartilage of P3 mice by digestion with collagenase. Mouse chondrocytes were cultured in DMEM with 10% fetal bovine serum (FBS) at 37°C. dsRNA oligonucleotides (5 nM) representing mature sequences that mimic endogenous miR-140 and Silencer Negative Control siRNA #1 (Ambion) were transfected into chondrocytes with Lipofectamine 2000 (Invitrogen). The synthesized RNA oligonucleotides 5′-CAGUGGUUUUACCCUAUGGUAG-3′ and 5′-ACCACAGGGUAGAACCACGGAC-3′ were annealed to obtain ds-miR-140. Silencer Negative Control siRNA #1 (siNega) was used at the same concentration as the specific miR-140 ds RNA in each experiment.

Luciferase assay

To create the pLuc2 reporter vector, a luciferase 2 gene (Promega) was incorporated into a modified pGL3-control plasmid with HindIII and EcoRI. To create the pGL3-miR-140 sensor vector (miR-140 sensor), the following chemically synthesized miR-140 multiple target sites were annealed and inserted between EcoRI and XhoI sites downstream from the firefly luciferase coding region in a pGL3 luciferase reporter plasmid with a modified 3′ UTR sequence (sense strand, 5′-AATTCTACCATAGGGTAAAACCACTGCTACCATAGGGTAAAACCACTGCTACCATAGGGTAAAACCACTG-3′; antisense strand, 5′-TCGACAGTGGTTTTACCCTATGGTAGCAGTGGTTTTACCCTATGGTAGCAGTGGTTTTACCCTATGGTAG-3′). To create the pLuc2-*Adamts-5* 3′ UTR vector (*Adamts-5* 3′ UTR), a fragment of the 3′ UTR of *Adamts-5* gene including the predicted miR-140-binding site was PCR-amplified using the primer set 5′-TGAATTCCTACTCTGCTTCCCTCTATGATC-3′ and 5′-TTCTCGAGCTGTGTTTCTTTCCTCAGGAG-3′, and then cloned downstream from the luciferase 2 gene with EcoRI and XhoI. To create the reporter vector with mutated miR-140-binding site (*Adamts-5* mut 3′ UTR), the 3′ UTR of *Adamts-5* was amplified with the primer set 5′-TGAATTCCTACTCTGCTTCCCTCTATGATC-3′ and 5′-CCCTCTAGACATAGATTTGACGAATATCCGTTTACCCTCCTTAGG-3′, and then cloned into a *Adamts5* 3′ UTR-containing vector with EcoRI and XbaI. ds-miR-140 and the scrambled siRNA sequences (AGUUGCACGCGCAAUUAdCdC and UAAUUGCGCGUGCAACUdTdT; final concentration, 50 nM) were reverse-transfected with Lipofectamine RNAiMAX (Invitrogen) into HEK293T cells (2.0×10^4 cells per well in a 96-well plate). After 24 h of transfection, culture medium was changed, and the firefly luciferase reporter plasmid (20 ng) and Renilla luciferase control plasmid pRL-SV40 (20 ng) were transfected with Lipofectamine 2000 (Invitrogen). Luciferase activity was determined with the Dual-Glo Luciferase Assay System (Promega).

Statistical analysis

Two-tailed independent Student's t-test and the nonparametric Wilcoxon signed-rank test were used for statistical analysis. Asterisks indicate differences with statistical significance at $P < 0.05$ (*) and $P < 0.01$ (**).

Acknowledgments

We thank E. Kim for her excellent technical support, and extend our gratitude to all other members in the laboratory. We also thank Y. Takahashi and M. Asada for their bioinformatics assistance, and E. Lamar for critical reading of the manuscript and discussion. T.S. and H.A. are associate scientists of Tokyo Medical and Dental University. This project was supported by NIH AR050631 (to H.A.), AR056120 (to H.A.), AG007996 (to M.K.L.), and AG033409 (to M.K.L.); the Arthritis National Research Foundation (S.M.); the Arthritis Foundation (S.O.); grants from the Ministry of Health, Labour, and Welfare; the Genome Network Project (MEXT); grants-in-aid for Scientific Research (MEXT); and grants from National Institute of Biomedical Innovation, Research on Child Health and Development, and The Japan Health Sciences Foundation.

References

Akiyama H. 2008. Control of chondrogenesis by the transcription factor Sox9. *Mod Rheumatol* **18:** 213–219.

Bartel DP. 2004. MicroRNAs: Genomics, biogenesis, mechanism, and function. *Cell* **116:** 281–297.

Downloaded from genesdev.cshlp.org on June 8, 2010 - Published by Cold Spring Harbor Laboratory Press

Chambers MG, Cox L, Chong L, Suri N, Cover P, Bayliss MT, Mason RM. 2001. Matrix metalloproteinases and aggrecanases cleave aggrecan in different zones of normal cartilage but colocalize in the development of osteoarthritic lesions in STR/ort mice. *Arthritis Rheum* **44:** 1455–1465.

de Crombrugghe B, Lefebvre V, Behringer RR, Bi W, Murakami S, Huang W. 2000. Transcriptional mechanism of chondrocyte differentiation. *Matrix Biol* **19:** 389–394.

Elia L, Quintavalle M, Zhang J, Contu R, Cossu L, Latronico MV, Peterson KL, Indolfi C, Catalucci D, Chen J, et al. 2009. The knockout of miR-143 and -145 alters smooth muscle cell maintenance and vascular homeostasis in mice: Correlates with human disease. *Cell Death Differ* **16:** 1590–1598.

Glasson SS, Askew R, Sheppard B, Carito BA, Blanchet T, Ma HL, Flannery CR, Kanki K, Wang E, Peluso D, et al. 2004. Characterization of and osteoarthritis susceptibility in ADAMTS-4-knockout mice. *Arthritis Rheum* **50:** 2547–2558.

Glasson SS, Askew R, Sheppard B, Carito B, Blanchet T, Ma HL, Flannery CR, Peluso D, Kanki K, Yang Z, et al. 2005. Deletion of active ADAMTS5 prevents cartilage degradation in a murine model of osteoarthritis. *Nature* **434:** 644–648.

Glasson SS, Blanchet TJ, Morris EA. 2007. The surgical destabilization of the medial meniscus (DMM) model of osteoarthritis in the 129/SvEv mouse. *Osteoarthritis Cartilage* **15:** 1061–1069.

Goldring MB, Goldring SR. 2007. Osteoarthritis. *J Cell Physiol* **213:** 626–634.

Goldring MB, Marcu KB. 2009. Cartilage homeostasis in health and rheumatic diseases. *Arthritis Res Ther* **11:** 224. doi: 10.1186/ar2592.

Harfe BD, McManus MT, Mansfield JH, Hornstein E, Tabin CJ. 2005. The RNaseIII enzyme Dicer is required for morphogenesis but not patterning of the vertebrate limb. *Proc Natl Acad Sci* **102:** 10898–10903.

Hashimoto M, Nakasa T, Hikata T, Asahara H. 2008. Molecular network of cartilage homeostasis and osteoarthritis. *Med Res Rev* **28:** 464–481.

Iliopoulos D, Malizos KN, Oikonomou P, Tsezou A. 2008. Integrative microRNA and proteomic approaches identify novel osteoarthritis genes and their collaborative metabolic and inflammatory networks. *PLoS One* **3:** e3740. doi: 10.1371/journal.pone.0003740.

Kobayashi T, Lu J, Cobb BS, Rodda SJ, McMahon AP, Schipani E, Merkenschlager M, Kronenberg HM. 2008. Dicer-dependent pathways regulate chondrocyte proliferation and differentiation. *Proc Natl Acad Sci* **105:** 1949–1954.

Krebsbach PH, Nakata K, Bernier SM, Hatano O, Miyashita T, Rhodes CS, Yamada Y. 1996. Identification of a minimum enhancer sequence for the type II collagen gene reveals several core sequence motifs in common with the link protein gene. *J Biol Chem* **271:** 4298–4303.

Lewis BP, Burge CB, Bartel DP. 2005. Conserved seed pairing, often flanked by adenosines, indicates that thousands of human genes are microRNA targets. *Cell* **120:** 15–20.

Lim LP, Lau NC, Garrett-Engele P, Grimson A, Schelter JM, Castle J, Bartel DP, Linsley PS, Johnson JM. 2005. Microarray analysis shows that some microRNAs downregulate large numbers of target mRNAs. *Nature* **433:** 769–773.

Lin AC, Seeto BL, Bartoszko JM, Khoury MA, Whetstone H, Ho L, Hsu C, Ali AS, Alman BA. 2009. Modulating hedgehog signaling can attenuate the severity of osteoarthritis. *Nat Med* **15:** 1421–1425.

Liu N, Bezprozvannaya S, Williams AH, Qi X, Richardson JA, Bassel-Duby R, Olson EN. 2008. microRNA-133a regulates cardiomyocyte proliferation and suppresses smooth muscle gene expression in the heart. *Genes Dev* **22:** 3242–3254.

Malfait AM, Liu RQ, Ijiri K, Komiya S, Tortorella MD. 2002. Inhibition of ADAM-TS4 and ADAM-TS5 prevents aggrecan degradation in osteoarthritic cartilage. *J Biol Chem* **277:** 22201–22208.

Mankin HJ. 1971. Biochemical and metabolic aspects of osteoarthritis. *Orthop Clin North Am* **2:** 19–31.

Miyaki S, Nakasa T, Otsuki S, Grogan SP, Higashiyama R, Inoue A, Kato Y, Sato T, Lotz MK, Asahara H. 2009. MicroRNA-140 is expressed in differentiated human articular chondrocytes and modulates interleukin-1 responses. *Arthritis Rheum* **60:** 2723–2730.

Nakasa T, Miyaki S, Okubo A, Hashimoto M, Nishida K, Ochi M, Asahara H. 2008. Expression of microRNA-146 in rheumatoid arthritis synovial tissue. *Arthritis Rheum* **58:** 1284–1292.

Stanczyk J, Pedrioli DM, Brentano F, Sanchez-Pernaute O, Kolling C, Gay RE, Detmar M, Gay S, Kyburz D. 2008. Altered expression of microRNA in synovial fibroblasts and synovial tissue in rheumatoid arthritis. *Arthritis Rheum* **58:** 1001–1009.

Stanton H, Rogerson FM, East CJ, Golub SB, Lawlor KE, Meeker CT, Little CB, Last K, Farmer PJ, Campbell IK, et al. 2005. ADAMTS5 is the major aggrecanase in mouse cartilage in vivo and in vitro. *Nature* **434:** 648–652.

Stefani G, Slack FJ. 2008. Small non-coding RNAs in animal development. *Nat Rev Mol Cell Biol* **9:** 219–230.

Thirunavukkarasu K, Pei Y, Wei T. 2007. Characterization of the human ADAMTS-5 (aggrecanase-2) gene promoter. *Mol Biol Rep* **34:** 225–231.

Tuddenham L, Wheeler G, Ntounia-Fousara S, Waters J, Hajihosseini MK, Clark I, Dalmay T. 2006. The cartilage specific microRNA-140 targets histone deacetylase 4 in mouse cells. *FEBS Lett* **580:** 4214–4217.

Ueta C, Iwamoto M, Kanatani N, Yoshida C, Liu Y, Enomoto-Iwamoto M, Ohmori T, Enomoto H, Nakata K, Takada K, et al. 2001. Skeletal malformations caused by overexpression of Cbfa1 or its dominant negative form in chondrocytes. *J Cell Biol* **153:** 87–100.

Valencia-Sanchez MA, Liu J, Hannon GJ, Parker R. 2006. Control of translation and mRNA degradation by miRNAs and siRNAs. *Genes Dev* **20:** 515–524.

van Rooij E, Sutherland LB, Liu N, Williams AH, McAnally J, Gerard RD, Richardson JA, Olson EN. 2006. A signature pattern of stress-responsive microRNAs that can evoke cardiac hypertrophy and heart failure. *Proc Natl Acad Sci* **103:** 18255–18260.

van Rooij E, Sutherland LB, Qi X, Richardson JA, Hill J, Olson EN. 2007. Control of stress-dependent cardiac growth and gene expression by a microRNA. *Science* **316:** 575–579.

Vega RB, Matsuda K, Oh J, Barbosa AC, Yang X, Meadows E, McAnally J, Pomajzl C, Shelton JM, Richardson JA, et al. 2004. Histone deacetylase 4 controls chondrocyte hypertrophy during skeletogenesis. *Cell* **119:** 555–566.

Wienholds E, Kloosterman WP, Miska E, Alvarez-Saavedra E, Berezikov E, de Bruijn E, Horvitz HR, Kauppinen S, Plasterk RH. 2005. MicroRNA expression in zebrafish embryonic development. *Science* **309:** 310–311.

Xiao C, Rajewsky K. 2009. MicroRNA control in the immune system: Basic principles. *Cell* **136:** 26–36.

Yamasaki K, Nakasa T, Miyaki S, Ishikawa M, Deie M, Adachi N, Yasunaga Y, Asahara H, Ochi M. 2009. Expression of microRNA-146a in osteoarthritis cartilage. *Arthritis Rheum* **60:** 1035–1041.

Yokoyama S, Ito Y, Ueno-Kudoh H, Shimizu H, Uchibe K, Albini S, Mitsuoka K, Miyaki S, Kiso M, Nagai A., et al. 2009. A systems approach reveals that the myogenesis genome

Downloaded from genesdev.cshlp.org on June 8, 2010 - Published by Cold Spring Harbor Laboratory Press

network is regulated by the transcriptional repressor RP58. *Dev Cell* **17:** 836–848.

Zemmyo M, Meharra EJ, Kuhn K, Creighton-Achermann L, Lotz M. 2003. Accelerated, aging-dependent development of osteoarthritis in α1 integrin-deficient mice. *Arthritis Rheum* **48:** 2873–2880.

Zhao Y, Ransom JF, Li A, Vedantham V, von Drehle M, Muth AN, Tsuchihashi T, McManus MT, Schwartz RJ, Srivastava D. 2007. Dysregulation of cardiogenesis, cardiac conduction, and cell cycle in mice lacking miRNA-1-2. *Cell* **129:** 303–317.

Zhou G, Garofalo S, Mukhopadhyay K, Lefebvre V, Smith CN, Eberspaecher H, de Crombrugghe B. 1995. A 182 bp fragment of the mouse pro α 1(II) collagen gene is sufficient to direct chondrocyte expression in transgenic mice. *J Cell Sci* **108:** 3677–3684.

The *Mohawk* homeobox gene is a critical regulator of tendon differentiation

Yoshiaki Ito[a], Naoya Toriuchi[a], Teruhito Yoshitaka[a], Hiroe Ueno-Kudoh[a], Tempei Sato[a], Shigetoshi Yokoyama[a], Keiichiro Nishida[b], Takayuki Akimoto[c], Michiko Takahashi[a], Shigeru Miyaki[a], and Hiroshi Asahara[a,1]

[a]Department of Systems BioMedicine, National Research Institute for Child Health and Development, Tokyo 157-8535, Japan; [b]Department of Human Morphology, Science of Functional Recovery and Reconstruction, Okayama University Graduate School of Medicine and Dentistry, Okayama 700-8558, Japan; and [c]Laboratory of Regenerative Medical Engineering, Center for Disease Biology and Integrative Medicine, Graduate School of Medicine, University of Tokyo, Tokyo 113-0033, Japan

Edited* by Marc R. Montminy, The Salk Institute for Biological Studies, La Jolla, CA, and approved May 5, 2010 (received for review January 20, 2010)

***Mohawk* (*Mkx*) is a member of the Three Amino acid Loop Extension superclass of atypical homeobox genes that is expressed in developing tendons. To investigate the in vivo functions of Mkx, we generated *Mkx*$^{-/-}$ mice. These mice had hypoplastic tendons throughout the body. Despite the reduction in tendon mass, the cell number in tail tendon fiber bundles was similar between wild-type and *Mkx*$^{-/-}$ mice. We also observed small collagen fibril diameters and a down-regulation of type I collagen in *Mkx*$^{-/-}$ tendons. These data indicate that Mkx plays a critical role in tendon differentiation by regulating type I collagen production in tendon cells.**

Tendons are dense, fibrous connective tissues that connect muscle to bone, transmitting the forces that allow for body movement (1). Tendon damage from overuse or degeneration due to aging is a common clinical problem because damaged tendon tissue heals very slowly and rarely recovers completely (2). The establishment of new therapies, such as regenerative medicine, for injured tendons has been delayed by a limited understanding of tendon biology (1, 3).

Tendons are composed primarily of collagen fibrils that cross-link to each other to form fibers (4). A small number of tendon cells reside between parallel chains of these fibrils and synthesize the specific ECM that contains collagens and proteoglycans (4, 5). The elasticity of tendons is provided by the large amount of collagen, predominantly type I collagen and small amounts of other collagens, including types III, IV, V, and VI (4, 6–9). The proteoglycans found in tendons, including decorin, fibromodulin, biglycan, and lumican, act to lubricate and organize collagen fiber bundles (4, 5). Targeted disruption of these proteoglycans in mice leads to abnormal collagen fibrils in tendons (3, 10–13). Tendon disruptions have also been described in patients with defects in collagen production, such as Ehlers-Danlos Syndrome, in which the type I collagen gene is mutated (14). These studies indicate that the ability of tendon cells to produce ECM is important for tendon formation.

Recently, it was reported that *Scleraxis* (*Scx*), a basic helix–loop–helix (bHLH) transcription factor expressed in the tendon progenitors and cells of all tendon tissues (15, 16), is essential for tendon differentiation. *Scx* knockout mice show severe disruption of force-transmitting tendons, although ligaments, which are tissues connecting bone to bone that closely resemble tendons in their components, and short-range anchoring tendons are not affected (17). It was also reported that Scx positively regulates the expression of type I collagen, a main ECM component of tendons (18). However, the type I collagen does not completely disappear from the tendons of *Scx* knockout mice (17), suggesting the presence of other regulatory factors for type I collagen. The tendon differentiation mechanisms remain largely unknown, with Scx being the only known transcription factor regulating tendon differentiation.

Mohawk (*Mkx*; also known as *Irx1*) is the sole member of a newly characterized class within the Three Amino acid Loop Extension (TALE) superclass of atypical homeobox genes (19). These transcription factors are essential for a large set of developmental processes, including cell proliferation, differentiation, and positional specification (20–24). Initial characterization of mouse *Mkx* revealed a dynamic transcription pattern restricted to progenitors of tendon, skeletal muscle, and cartilage, as well as the sex chords of the male gonad and the ureteric bud tip of the metanephrogenic kidney (19, 25, 26). We previously identified *Mkx* as a transcription factor expressed in developing tendons by constructing a whole-mount in situ hybridization database, termed "EMBRYS" (http://embrys.jp/embrys/html/MainMenu.html), which contains expression data of 1,520 transcription factors and cofactors expressed in E9.5, E10.5, and E11.5 mouse embryos (27).

To investigate the in vivo functions of Mkx, we generated *Mkx* knockout mice. Here, we show that *Mkx* null mice have hypoplastic tendons throughout their body. Although the size of tendons is drastically reduced in *Mkx* null mice, the cell number in tail tendon fiber bundles shows no significant difference between wild-type and *Mkx* null mice. We also observed abnormal collagen fibrils in *Mkx* null tendons. Furthermore, we show that the expression of type I collagen, which is a major tendon ECM component, is down-regulated in the Achilles tendon of *Mkx* null mice. These data indicate that Mkx is a transcription factor controlling tendon differentiation by regulating type I collagen production in tendon cells.

Results

Generation of *Mkx* Mutant Mice. We inactivated the *Mkx* gene by homologous recombination in ES cells using a targeting vector to replace the *Mkx* gene from the start of translation to the end of exon 2 with the Venus gene and PGK-neomycin-resistance (PGK-neo) cassette (Fig. 1*A*). We predicted that the Venus gene, an improved GFP gene (28), would be expressed in *Mkx* positive cells in heterozygous mice generated with the targeting construct. We identified two correctly targeted ES cell clones by Southern blot analysis (Fig. S1 *A* and *B*). These two clones were microinjected into 8-cell stage embryos and germ-line transmission in the resulting chimeric mice was confirmed by Southern blotting and genomic PCR (Fig. 1*B* and Fig. S1*C*). *Mkx*$^{+/-}$ embryos showed robust Venus expression that recapitulated *Mkx* expression faithfully at E13.5 forelimb and tail (Fig. 1*C*). Also, these *Venus* knockin heterozygous mice showed tendon-specific Venus expression in the tail of E16.5 embryos (Fig. 1*D*). In addition to embryos, we investigated Venus expression in adult mice. Because Mkx expression in tendons of adult mice had not been determined, we analyzed

Author contributions: Y.I., S.Y., and H.A. designed research; Y.I., N.T., T.Y., H.U.-K., T.S., S.Y., K.N., T.A., M.T., and H.A. performed research; Y.I., H.U.-K., T.S., and H.A. contributed new reagents/analytic tools; Y.I., N.T., T.Y., S.Y., K.N., T.A., S.M., and H.A. analyzed data; and Y.I. and H.A. wrote the paper.

The authors declare no conflict of interest.

*This Direct Submission article had a prearranged editor.

Freely available online through the PNAS open access option.

[1]To whom correspondence should be addressed. E-mail: asahara@nch.go.jp.

This article contains supporting information online at www.pnas.org/lookup/suppl/doi:10.1073/pnas.1000525107/-/DCSupplemental.